



OPEN

SUBJECT AREAS:

COMPUTATIONAL
MODELS

BIOCHEMICAL NETWORKS

NETWORK TOPOLOGY

SYSTEMS ANALYSIS

Received
29 April 2013Accepted
26 July 2013Published
28 August 2013Correspondence and
requests for materials
should be addressed toJ.N. (nielsenj@
chalmers.se)

Understanding the interactions between bacteria in the human gut through metabolic modeling

Saeed Shoaie, Fredrik Karlsson, Adil Mardinoglu, Intawat Nookaew, Sergio Bordel & Jens Nielsen

Department of Chemical and Biological Engineering, Chalmers University of Technology, SE412 96 Gothenburg, Sweden.

The human gut microbiome plays an influential role in maintaining human health, and it is a potential target for prevention and treatment of disease. Genome-scale metabolic models (GEMs) can provide an increased understanding of the mechanisms behind the effects of diet, the genotype-phenotype relationship and microbial robustness. Here we reconstructed GEMs for three key species, (*Bacteroides thetaiotamicron*, *Eubacterium rectale* and *Methanobrevibacter smithii*) as relevant representatives of three main phyla in the human gut (Bacteroidetes, Firmicutes and Euryarchaeota). We simulated the interactions between these three bacteria in different combinations of gut ecosystems and compared the predictions with the experimental results obtained from colonization of germ free mice. Furthermore, we used our GEMs for analyzing the contribution of each species to the overall metabolism of the gut microbiota based on transcriptome data and demonstrated that these models can be used as a scaffold for understanding bacterial interactions in the gut.

The gut microbiota functions as a metabolically active organ and digests dietary components that are indigestible for human cells which can then be absorbed and metabolized by the human body¹. The gut microbiota is also involved in the stimulation of the immune system and in providing resistance to pathogens. Perturbation or diversion of the metabolic functions carried out in the gut microbiota can lead to the development of different disorders². Metagenomic studies have shown that the gut microbiome is associated with human diseases such as obesity³, type 2 diabetes^{4,5} and atherosclerosis⁶, and the composition of the gut microbiota has been shown to be influenced by the diet, environment and age⁷.

Improvements in DNA sequencing technology and cost reductions open new possibilities to study the human microbiome in health and disease. 16S rRNA sequencing has indicated that the gut microbiota is mainly dominated by the phyla Bacteroidetes (17–60%) and Firmicutes (35–80%)^{8,9}. Other key phyla in the human gut microbiota are Actinobacteria, Proteobacteria and Euryarchaeota^{6,10}. Previous studies have shown that Firmicutes are increased and Bacteroidetes are decreased in obese mouse models¹¹. Better understanding of the interactions between these phyla as well as with the host may provide valuable insights into the underlying mechanisms of the different disorders. These interactions can be mediated by the production of short chain fatty acids (SCFAs) (acetate, propionate and butyrate), hydrogen and methane which are of potential interests in our study.

The SCFAs absorbed through the gut epithelial cells, have strong effects on the energy regulation and the immune system of the host¹². The relative absorption of SCFAs by the colon varies between 60–90%^{13,14}, and oxidation of SCFAs can provide energy for colonic mucosa and may contribute up to 5–10% of the total energy in a healthy body¹⁵. Acetate is the main SCFA in the blood and plays a key metabolic role for peripheral tissues being a substrate for lipogenesis and cholesterol synthesis and propionate is the precursor preferred by the liver to regulate cholesterol synthesis and gluconeogenesis¹². The other SCFA, butyrate is an important energy source for colonocytes and affects the human energy balance by influencing energy regulation¹². Butyrate is used as a fuel metabolite by colonocytes, resulting in a high level of ATP production¹⁶. Additionally, it has been recently proven that butyrate has protective roles against colon carcinogenesis¹⁷. Different studies have shown that absorbed butyrate in the colonocyte, inhibits histone deacetylase which modulates the colorectal cancer cell lines growth by influencing apoptosis, cell proliferation and differentiation^{17–20}.

The bacterial fermentation and the production of SCFAs in the human gut are strongly associated with the dietary pattern which is correlated with the composition of bacteria in the gut. Modulation of the gut microbiota



composition and the diet have been characterized both in human and animal studies^{21,22}. Gnotobiotic mice harboring ten sequenced bacteria have been used to study the effect of different diets on species abundance and gene expression. A statistical method was developed for prediction of the bacterial abundance and identification of important factors in each diet²³.

In order to obtain an increased understanding of the complex interactions between diet, microbiota and the host phenotype, reconstruction of genome-scale metabolic models (GEMs) for representative species of abundant phyla in the gut microbiota can provide an integrative platform to bridge the gap between genotype and phenotype²⁴. GEMs are collection of biochemical reactions that occur in an organism, reconstructed based on high throughput omics data and known biochemical reactions which provide a scaffold for the analysis of such data^{25,26}. GEMs can be employed to evaluate factors that result in modulation of the gut microbiota metabolism, and eventually to design clinical interventions²⁷.

Previously, the mutualistic interactions between two bacteria have been studied through stoichiometric constraint based modeling²⁸. This study represented the first attempt to simulate the interplay between microbial communities by considering each metabolic network as a separate compartment. This was followed by a multilevel optimization framework for the metabolic modeling and analysis of microbial communities called OptCom²⁹. These two approaches constitute a framework for simulating ecosystems, but these approaches have not been applied and adapted to model the human gut microbiota³⁰.

Here, we used two recently available technologies including genome scale modeling and meta-omics for describing the metabolism in the gut ecosystem and its interactions with the host. Two well characterized bacteria, *Bacteroides thetaiotamicron* (*iBth1201*) and *Eubacterium rectale* (*iEre400*) as representatives of the two abundant phyla, Bacteroides and Firmicutes respectively, were chosen for GEM reconstruction. *Methanobrevibacter smithii* (*iMsi385*), as a methanogenic and dominant archaeon in the human gut microbiome was selected as a third species because it plays a key role in gut microbial metabolism of hydrogen³¹. Despite of low abundance of *M. smithii* in metagenomics studies, it has a significant role in the human gut by removal of hydrogen gas and production of methane. Removal of hydrogen gas is important to consider as it affects bacterial fermentation and energy harvesting³².

Each GEM was validated using experimentally observed data and used for simulations of a simplified gut ecosystem. During our simulations, we formalized mathematically two different scenarios and applied them for modeling of gut microbiota. In the first case, the composition of the diet and the species abundances in the microbiota are known and constitute the input of the model. We predicted the profile of compounds produced by the microbiota and hence represented metabolites that can be taken up by the host. This simulation is referred as the α -problem and a solution was found by minimizing the substrate uptake rate (Figure 1). In the second case, which is referred as the β -problem, we predicted the abundances of the different species in the microbiota as a function of the diet. Next, we employed our GEMs for the analysis of transcriptomics data that profile the gene expression data of *Bacteroides thetaiotamicron* and *Eubacterium rectale* responds to each other³³ and identified the metabolic differences in each bacteria using Reporter Metabolites and Subnetworks³⁴. Furthermore we identified the transcriptionally regulated reactions using a random sampling algorithm³⁵. We provided a mechanistic interpretation to statistical findings provided by metagenomics through the integrating of gut ecosystem modeling, diet compositions, genomic and transcriptomic data (Figure 1). This leads to improved understanding of the relationships between diet, microbiota and host and hereby enables a rational design of prebiotic and probiotic treatments.

Results

GEMs reconstruction of three representative bacteria in the human gut microbiota. In order to reconstruct draft GEMs for *B. thetaiotamicron*, *E. rectale* and *M. smithii*, we first identified species for which GEMs have already been manually reconstructed using a bottom-up approach. This led us to choose well-studied template GEMs, *Escherichia coli* (*iAF1260*), *Staphylococcus aureus* (*iSB619*) and *Methanosarcina acetivorans* (*iVS941*) as templates species for *B. thetaiotamicron*, *E. rectale* and *M. smithii*, respectively^{36–38}. Due to different phylogeny of the template models and selected species, intensive manual curation was applied on the draft models based on literature and databases such as KEGG³⁹, BRENDA, and Seed models⁴⁰ for the identification and correction of inconsistencies. Biologically defined metabolic tasks that occur in each bacteria were defined and successful simulation of each task was completed using the RAVEN toolbox⁴¹. These metabolic tasks include the production of amino acids, nucleotides and carbohydrate metabolism and are summarized in Supplementary Dataset 1.

During the reconstruction process, we used genome sequences, previously published models and gene homology information as input (Figure 1). The homology information was obtained by performing a bidirectional BLASTp search between the organism of interest and the set of template organisms using standard settings. *iBth1201* was compared with recently published model for *B. thetaiotamicron* *iAH991*⁴² and it is observed that *iBth1201* includes all of the genes and associated reactions in *iAH991* as well as 210 additional genes. The predictions obtained through *iBth1201* were in agreement with *in-vitro* chemostat data⁴³ (Figure S1). The production of butyrate and the uptake of acetate and oligo and polysaccharides were predicted through *iEre400* and were in agreement with *in-vitro* experiments⁴⁴. Uptake of hydrogen, formate and acetate and production of methane were also predicted using *iMsi385*, which was also consistent with experimental observations⁴⁵. The characteristics of each GEM are summarized in table S1 and these GEMs are publicly available through the Human Metabolic Atlas web-site (www.metabolicatlas.com).

Solution of the α -problem in well-characterized gut ecosystems.

The α -problem is defined as the determination of the secretion profile of metabolites as a function of the diet and the species abundances. Here, we solved the α -problem in a well-characterized gut ecosystem by integrating data on microbial composition from the literature and predicting the metabolites produced. A well-characterized gut ecosystem is defined as a microbial community in which the substrates and fermentation products of each bacteria are known. The microbial abundances (translated into gram biomass/gram luminal content) were inferred from humanized gnotobiotic mouse models. The α -problem was solved by fixing the biomass content of each organism to its experimental value and minimizing the substrate uptake. The interactions with the human gut were also considered by introducing experimental diffusion coefficients through the gut wall⁴⁶. According to the available experimental designs, two different cases were simulated including single bacteria and the community of two microbial species. For both cases our simulation results were validated against experimental data^{33,47}.

In-silico evaluations of single species as a simple model for gut microbiome.

iBth1201 was used to predict the profile of SCFAs and other byproducts and these predictions were compared with observed profiles of SCFAs in mono-colonized germ-free mice (Figure 2A). Predictions for two SCFAs (propionate and acetate) concentrations were in agreement with the experimental data. The deviation for acetate predictions and experimental values was 7.5 $\mu\text{mol/g}$ Cecal and for propionate 1.5 $\mu\text{mol/g}$ Cecal, which correspond to 25% and 22% deviation from the experimental value

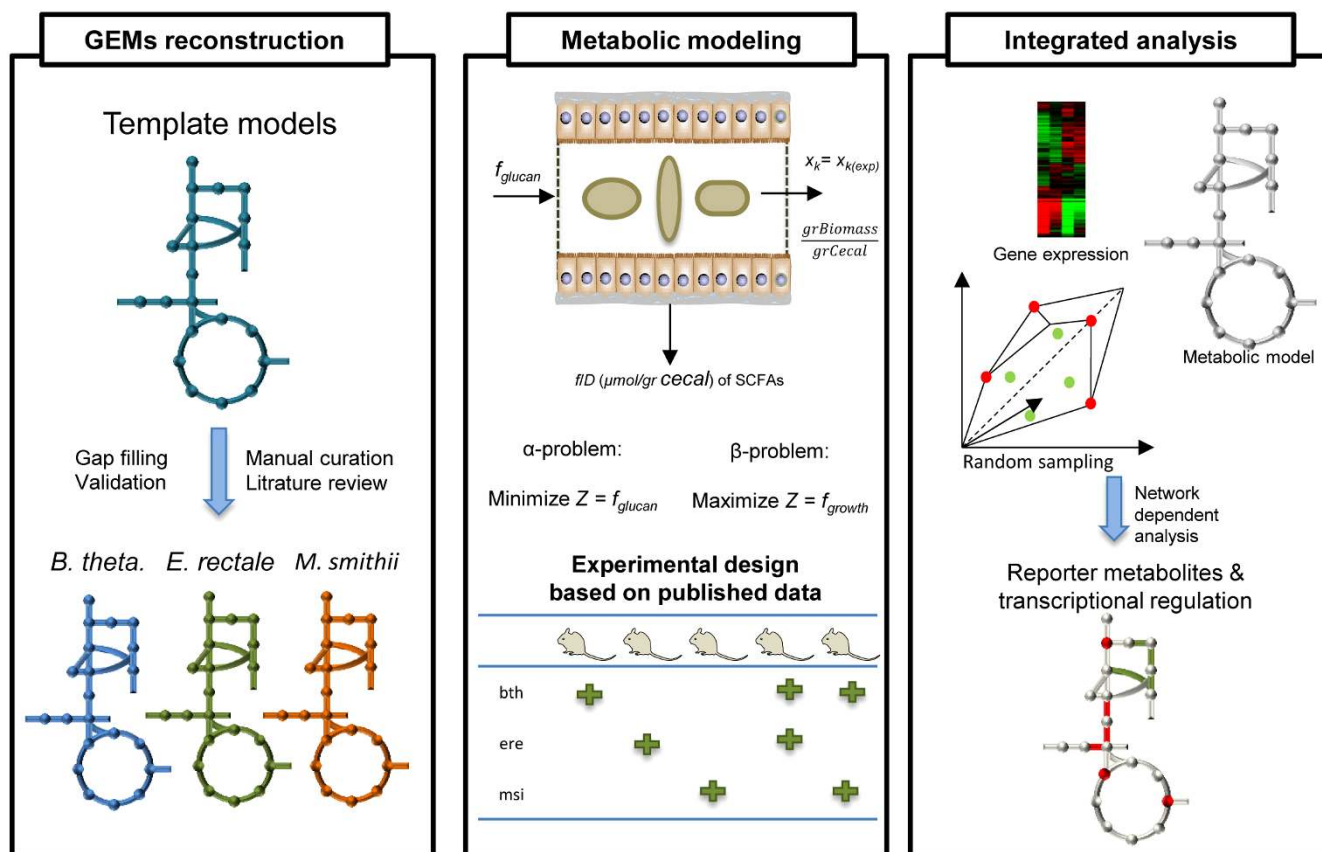


Figure 1 | Genome-scale metabolic models (GEMs) for gut microbiota are reconstructed based on three template models and different databases. This was followed by intensive manual curation of the GEMs for three key species in the human gut microbiome, based on literature and databases. The metabolic modeling step involved two approaches, the α - and β -problem which were defined depending on the availability of experimental data (the mono-colonization of germ free mice with *B. thetaiaotomicron*³³, *E. rectale*³³ and *M. smithii*²⁷, the co-colonization of germ free mice with the *B. thetaiaotomicron* and *E. rectale*³³, the *B. thetaiaotomicron* and *M. smithii*²⁷). In the α -problem the abundance of the species were specified and the glucan and the SCFAs uptake and secretion profile was predicted. For the β -problem, the concentration of substrates in the feed was specified and the biomass and the SCFAs profile were predicted. Finally, the metabolic differences between each bacteria were identified through integrative analysis. Reporter metabolites, subnetworks and random sampling algorithms were used to reveal information about transcription regulations based on the transcriptome data.

for acetate and propionate, respectively. Next *iEre400* was implemented as the sole gut bacterium and the concentration of butyrate, CO₂ and H₂ were predicted, and the results were compared with experimental data from colonization of germ-free mice with *E. rectale* (Figure 2B). The deviation between predicted and measured butyrate concentration was 0.07 $\mu\text{mol/g}$ Cecal corresponding to 40% deviation from the measured concentration. Finally *iMsi385* was implemented to predict the consumption of acetate and production of methane by using constraint-based modeling (Figure 3A), and the simulations showed consistency with experimentally determined methane production.

In-silico evaluations of two species ecosystems. Following evaluation of the individual models we simulated gut ecosystems involving two species. In the first case, when *E. rectale* is together with *B. thetaiaotomicron*, the main metabolite exchanged between the two organisms is acetate. In presence of *B. thetaiaotomicron*, *E. rectale* takes up small proportions of the acetate produced by *B. thetaiaotomicron* and convert it into butyrate. Very small proportions of carbohydrates are consumed by *E. rectale* and most are taken up by *B. thetaiaotomicron*. In order to model these interactions, the community stoichiometric matrix was built based on single stoichiometric matrixes. Here, the extracellular medium was treated as a common compartment between the two species. The same optimization formulation were implemented here (Figure 2D). The

biomass concentration of each of the species in the community was fixed to its experimental value and constraint-based modeling was employed to minimize the substrate uptake. The SCFAs profile was compared to experimental values, where the deviation for acetate, propionate and butyrate were 0.7 (14%), 1.2 (40%) and 0.07 (30%) $\mu\text{mol/g}$ Cecal, respectively (Figure 2C). In the second case the other combination of species, *B. thetaiaotomicron* and *M. smithii* was simulated. The main interactions between these two are the exchange of acetate and formate, which are taken up by *M. smithii* and ended up with production of methane by methanogenesis. Again in this case the biomass content of each community member was fixed to its experimental value. The secretion profile of the community was predicted as depicted in figure 3B by minimizing the substrate uptake rate and it was compared to the available experimental values. The deviation for acetate and propionate was 2.8 (40%) and 0.07 (14%) $\mu\text{mol/g}$ Cecal respectively and these were within the range of experimental measurements (Figure 3B). To examine how the key predictions correlate with assigned biomass values, robustness analysis was applied for production of SCFA and consumption of glucan with different constraints of biomass. We defined a sensitivity coefficient (the ratio of biomass and SCFAs production changes for different constraints) which was close to one. This means that the relative error in the biomass estimation is equal to the relative error in the SCFAs prediction (Figure S2 & S3). Besides, the errors in the measured biomass concentrations are

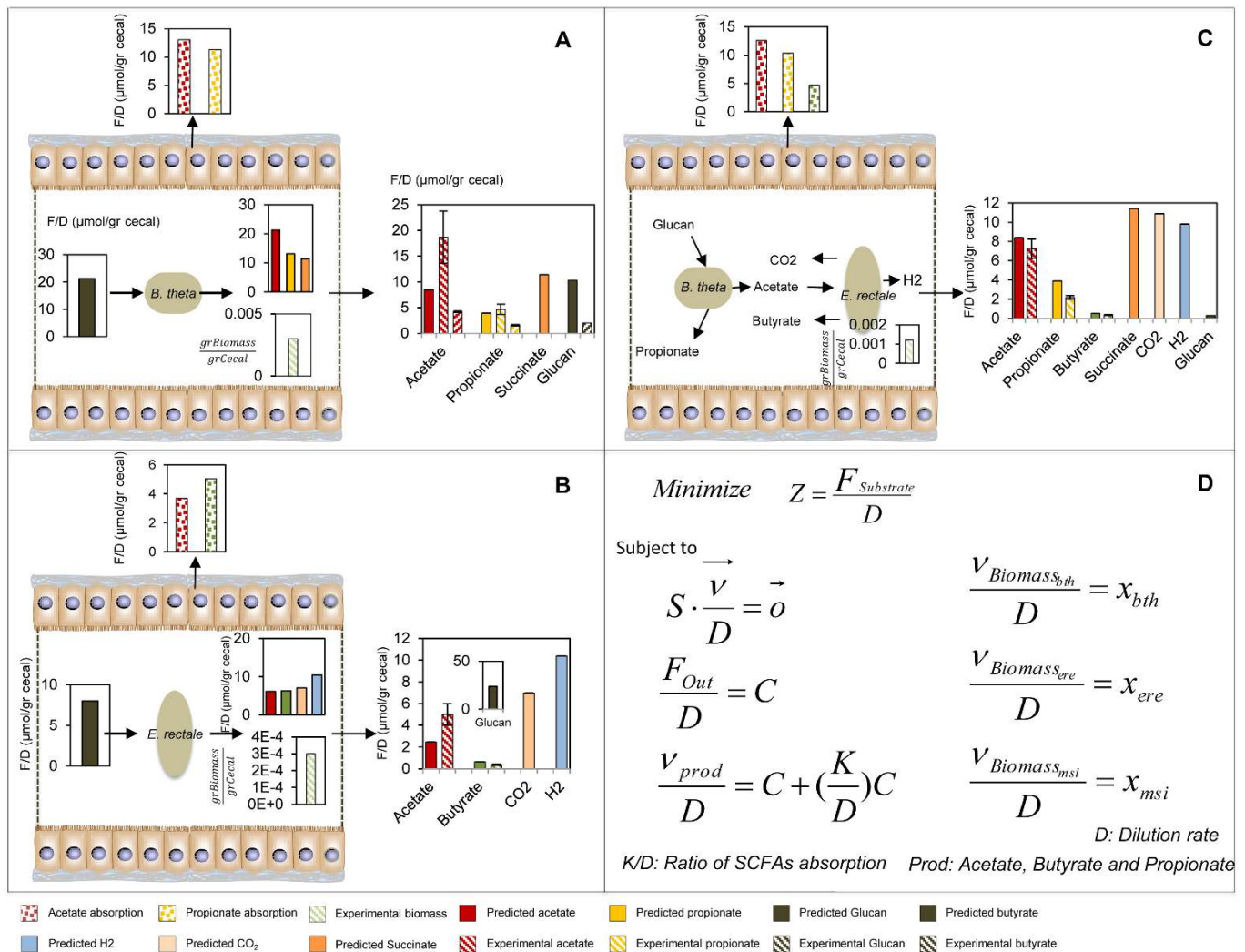


Figure 2 | Comparison of the experimental measurements and predictions obtained from the solution of the α -problem for the ecosystem composed of *B. theta* (A), *E. rectale* (B) and community of *B. theta* and *E. rectale* (C) in colonized germ free mice. The green bar for different simulations indicates the abundant of species in the ecosystem. The total amount of available glukan for mice and produced acetate were calculated based on available experimental data. The amounts of absorbed SCFAs by the epithelial cells and the concentrations of SCFAs in the feces are shown. (D) The formulation for solving the α -problem is presented. The experimental data was reported in concentrations per unit of cecal content hence all the metabolic fluxes were divided by specific production rate of cecal content. The output fluxes are formulated in concentrations using the objective function. For all cases the initial glukan and acetate values are 31 and 6 $\mu\text{mol/gr}$ cecal, respectively. The $x_{ere,msi,bth}$ is the biomass experimental value for each species. (All units are F/D ($\mu\text{mol/gr}$ cecal)).

over 20%, which explains the relative errors in the prediction of short chain fatty acids. On the other hand (Figure 2A) the discrepancy in the experimental measurements of short chain fatty acids for different biological replicates (different mice) is also very high. Our predictions are as good as the quality and accuracy of the available experimental data allow.

Solution to the β -problem for two and three species. The β -problem is defined as the prediction of both the biomass composition of the microbiota as well as the secretion profile of SCFAs with a known diet composition. The rational design of probiotics and prebiotics cannot be fully achieved without a methodology for solving the β -problem. Our *in-silico* method enabled testing the effects of different diets on the abundance of bacterial species present in the colon and their SCFAs secretion profile. The β -problem was solved for a community of *B. theta* and *M. smithii*, by fixing the uptake rate for glukan to 20 $\mu\text{mol/g}$ Cecal and maximizing the sum of biomass concentrations of *B. theta* and *M. smithii*. The observed predicted values for the abundance of each species, SCFAs and

methane production were in agreement with experimental data^{33,47}. The abundance of *B. theta* and *M. smithii* were 1.0 and 0.08 mg Biomass/g Cecal, respectively.

To achieve further insight into the metabolic function of the human gut microbiota, the interactions of three species as representatives of predominant phyla were investigated. Solving the β -problem for three species leads to identification of the diet leading to the optimum SCFAs production which is in correlation with abundances of *B. theta*, *E. rectale*, and *M. smithii* (Figure 4A). The inter-relationships of this simplified community were acetate production by *B. theta* and consumption by *E. rectale* and *M. smithii* as well as CO₂ production by *E. rectale* and consumption by *M. smithii*. The substrate was set and split between *E. rectale* and *B. theta* which was observed from simulations with the α -problem and the objective function was defined as total growth of the microbial community (Figure 4B). By solving this problem corresponding SCFAs, abundances of each member of community and other byproducts such as methane and succinate were predicted. The patterns of SCFAs in this three species community were

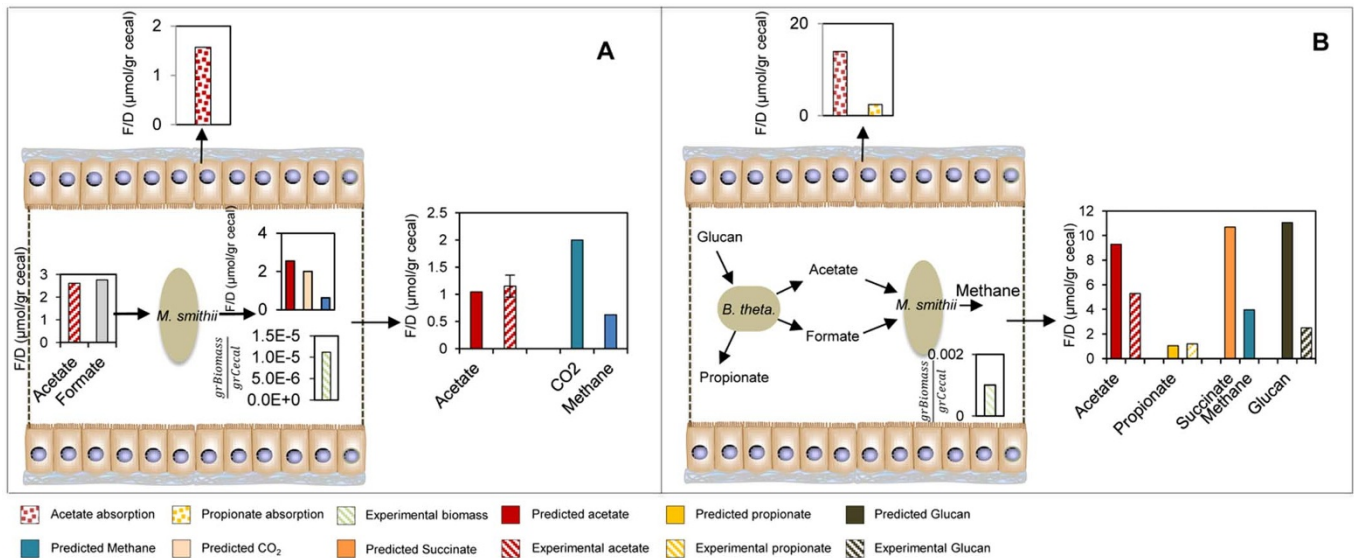


Figure 3 | Comparison of the experimental measurements and predictions obtained from the solution of the α -problem for the ecosystem composed of *M. smithii* (A) and community of *B. thetaiotaomicron* and *M. smithii* (B) in colonized germ-free mice. The results are compared with predictions obtained from the solution of the α -problem. For community simulation the initial glucan and acetate values are 31 and 6 $\mu\text{mol/gr cecal}$, respectively. (All units are F/D ($\mu\text{mol/gr cecal}$)).

observed to be similar to the patterns in community with *E. rectale* and *B. thetaiotaomicron* (Figure 4A). This conceptual modeling result is the most realistic case in the human gut microbiota where SCFAs were produced, hydrogen gas was taken up and methane was produced by the *M. smithii*. The robustness analysis was also applied for the β -problem, where different values for glucan were assigned as an input to the community and the SCFAs and biomass of the community were predicted. The sensitivity coefficient (*S*) for this simulation was also found to be close to one (Figure S4 & S5).

Integrative analysis of transcriptomic data for gut microbial communities. GEMs represent the link between genotype and phenotype and allow for generating testable hypothesis for cellular

metabolism and for drawing novel biological conclusions based on omics data. In this context, we used a transcriptome dataset³³ that profiled the transcriptome of *E. rectale* and *B. thetaiotaomicron* in monocolonized mice with a co-colonization of the two. We applied the reporter metabolites algorithm that identifies a set of metabolites around which there is observed a strong transcriptional response³⁴. By generating the GEMs for these three species, using published gene expression data and applying network dependent analysis we used transcriptome data to get more insight at the mechanistic level (metabolite and gene level). We identified reporter metabolites, subnetworks and transcriptional regulation which have not been reported in the previous study. The use of GEMs and reporter algorithms is much easier for metabolic interpretation than

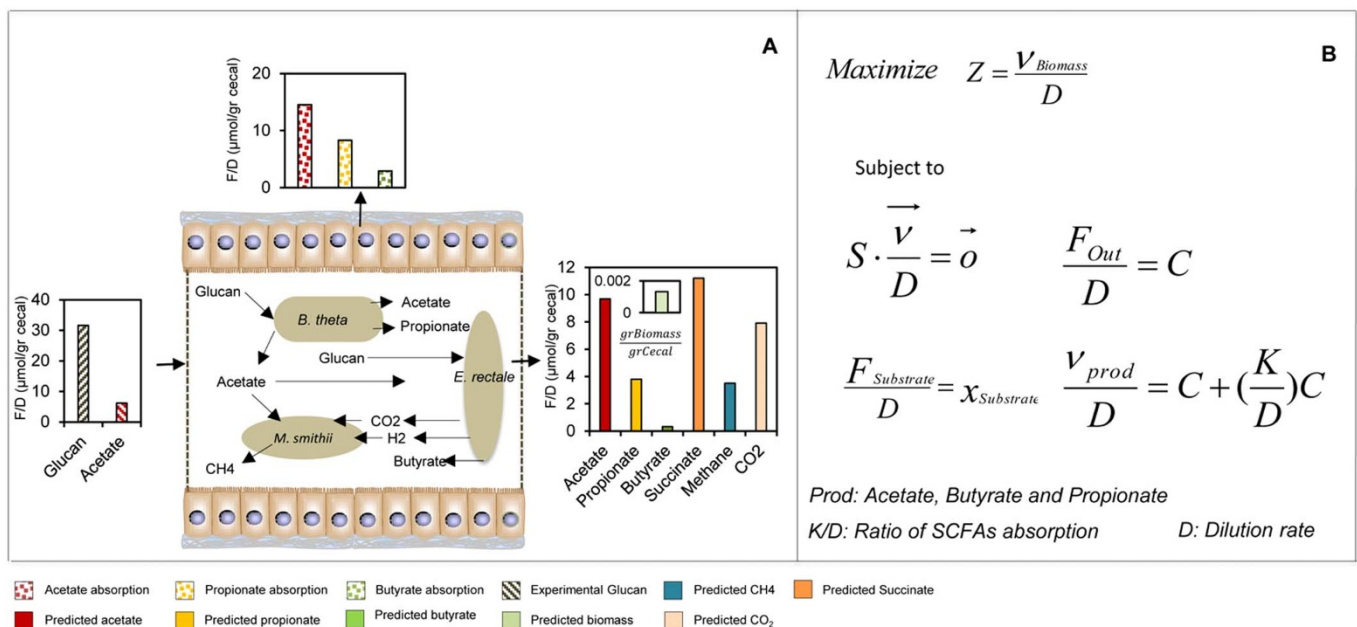


Figure 4 | (A) Predictions obtained from the solution of β -problem for the ecosystem composed of *B. thetaiotaomicron*, *E. rectale* and *M. smithii*. In this case, the biomass content of the community used as an objective function. The profiles for SCFAs productions were obtained based on available amount of glucan. (B) The formulation to solve the β -problem (All units are F/D ($\mu\text{mol/gr cecal}$)).



manual looking through a list of genes. We presented reporter metabolites for *E. rectale* during its adaptation to *B. thetaiotaomicron* (Figure 5A) and reporter metabolites for *B. thetaiotaomicron* during its adaptation to *E. rectale* (Figure 5B). The reporter metabolites linked to the up and down regulated genes are presented. The analysis revealed that *E. rectale* responded to the presence of *B. thetaiotaomicron* by up-regulating the genes around the metabolites involved in amino acid metabolism, aminoacyl-tRNA biosynthesis, TCA cycle, NAD and CoA synthesis and nucleotide synthesis. These findings were in agreement with Mahowald *et al.*³³. We also observed that there is significant down regulation of enzymes in carbohydrate metabolism, such as melibiose, fructose, galactose and raffinose (Figure 5A & Supplementary Dataset 2). It should also be noted that the expression of the genes encoding enzymes interacting with L-alanine, L-methionine and L-homocysteine changed in both directions. *B. thetaiotaomicron* responded to the presence of *E. rectale* by up-regulating the expression of genes around the poly and mono-saccharides, carbohydrates and glycans ((Figure 5B & Supplementary Dataset 3). We also found that genes linked to beta-alanine, L-cysteine and selenide are down regulated.

In order to gain more insights into the molecular mechanisms involved in the response of *B. thetaiotaomicron* and *E. rectale*, the reporter sub-network algorithm was applied to identify set of metabolic reactions which exhibit transcriptional correlation. The

identified reporter sub-networks are presented in figure 6 after removing highly connected metabolites (e.g. cofactors) (Supplementary Dataset 4 & 5). It is observed that *E. rectale* responds to *B. thetaiotaomicron* by increasing the utilization of amino acids and decreasing the degradation of carbohydrates (Figure 6A) whereas *B. thetaiotaomicron* responds to *E. rectale* by increasing the utilization of polysaccharides (Figure 6B). The complete reported subnetworks for both cases are presented in figure S6 & 7.

Revealing transcriptional regulation information. The regulatory mechanisms responsible for the changes in the distribution of metabolic fluxes between two states can be inferred using the GEMs by incorporating measured external fluxes and transcriptomic data in our random sampling algorithm³⁵. Here, we used external fluxes predicted based on the α -problems and calculated a set of possible distributions of internal fluxes consistent with the secretion profiles for each of the considered conditions. We first evaluated the response of *E. rectale* to the presence of *B. thetaiotaomicron* and this analysis revealed that *E. rectale* transcriptionally up regulated the flux in amino acid metabolism, in particular reactions involving glutamine, serine, glycine, methionine, isoleucine, arginine and citrulline. Pyruvate decarboxylation, pyruvate phosphotransferase, 2-phospho-D-glycerate hydro-lyase and H₂-oxidizing hydrogenase reactions were also identified as transcriptionally down -regulated (Supplementary Dataset 6). Reactions such as 2-aceto-2-hydroxybutanoate synthase

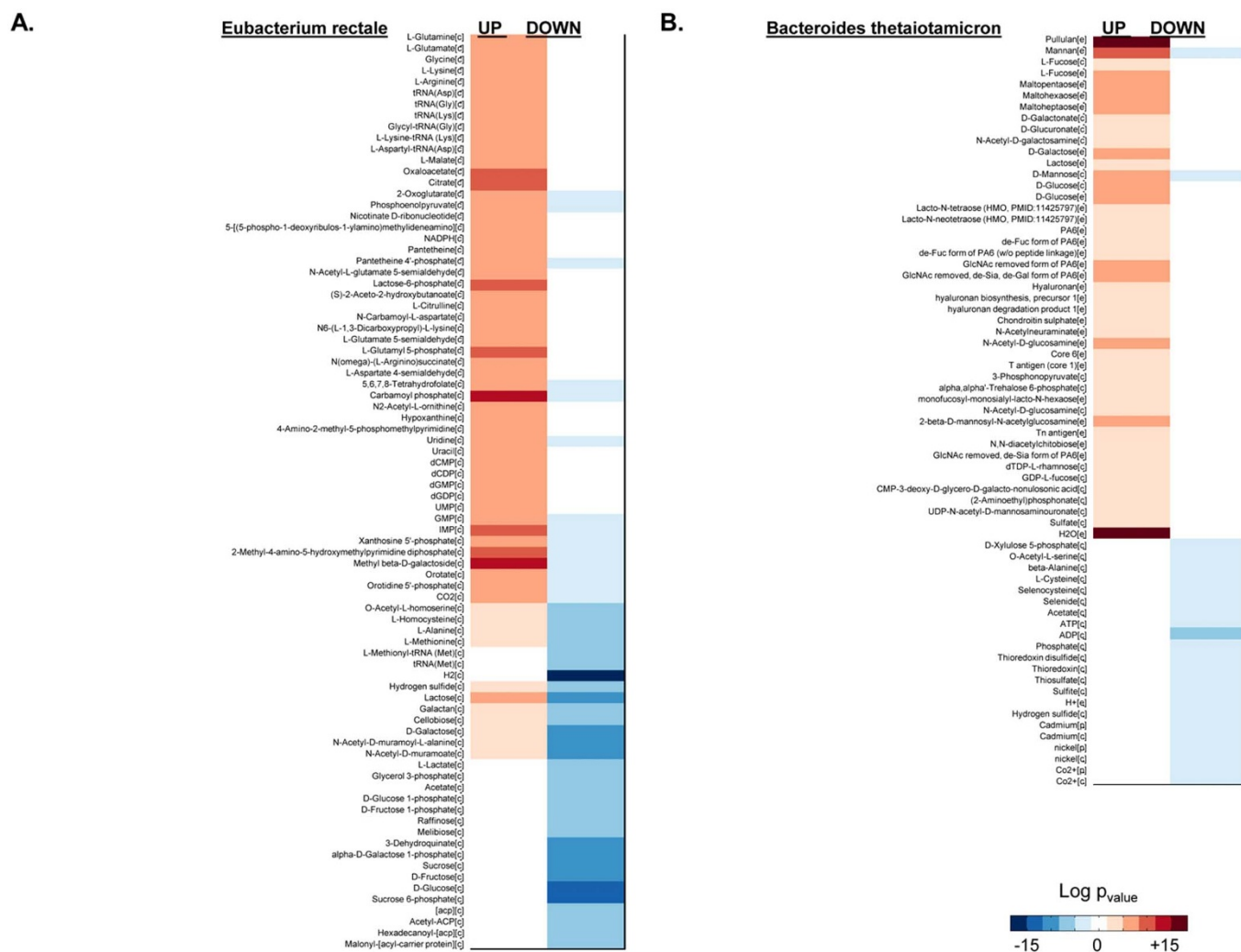


Figure 5 | The reporter metabolites were identified for two conditions based on colonic transcriptional data³³. (A) The response of *E. rectale* to *B. thetaiotaomicron* (B) response of *B. thetaiotaomicron* to *E. rectale*.



higher uptake of acetate. The response of the butyrate production to changes in glucan and acetate is depicted in figures S8 and S9.

Another sensitivity analysis was applied on a community of *E. rectale* and *B. thetaiotaomicron*. In this analysis, the abundances of *B. thetaiotaomicron* and *E. rectale* in the community were varied to check optimal production of butyrate. Figure S10 shows how the butyrate production increases with the increased abundance of *E. rectale*. As mentioned above, butyrate is a key component that affects energy homeostasis and functions as histone deacetylase inhibitor, which has a direct effect on colorectal cancer. The results of this analysis can propose a solution for finding the threshold of butyrate formation based on the abundances of Bacteroides and Firmicutes.

Discussion

In order to understand the function of bacteria in the human gut ecosystem and its interaction with the host, we reconstructed three GEMs, *iBth1201* (*B. thetaiotaomicron*), *iEre400* (*E. rectale*) and *iMsi385* (*M. smithii*), which are relevant representatives of three main phyla in the human gut (Bacteroidetes, Firmicutes and Euryarchaeota). We predicted the substrate uptake rates and the secreted SCFAs profiles for different combination of these three bacteria through *in silico* co-colonization of germ free mice. We simulated that the production of butyrate increased when *B. thetaiotaomicron* was co-colonized with *E. rectale*. This alteration of butyrate has different impacts on human health and it is involved in the progression of disorders such as colon cancer, diabetes and obesity^{17–20,48}. In the joint simulation of *B. thetaiotaomicron* and *M. smithii*, the acetate produced by *B. thetaiotaomicron* and consumed by *M. smithii* as well as methane produced by *M. smithii* was predicted. It was observed that methane production was also increased in the community of *M. smithii* and *B. thetaiotaomicron* compared to *M. smithii* as the sole bacteria. The predictions of SCFAs production were compared to experimental data and they were in agreement with experimental observations.

In order to simulate the metabolic effect of the gut species on the host metabolism, we used experimentally measured diffusion coefficients for the absorption of each SCFA by the epithelial cells. It should be noted that the diffusion coefficients of SCFAs can differ based on individual genetic differences as well as the health status of the host. For all simulations, we used a fixed value for the diffusion coefficients (Acetate 60%, Propionate 70% and Butyrate 90%) based on previous studies^{13,14}. We also demonstrated that it is possible to find the solution of the α -problem in well-characterized ecosystems where the exchange of metabolites by different bacteria is unknown a-priori. During our analysis, the exchange metabolites inferred from the structure of the metabolic models for the gut microbiota and the experimental biomass production of the species at minimal substrate consumption was simulated. The very good fit between our simulations and experimental data shows that the models correctly capture the electron balancing associated with the mixed acid fermentations occurring in the studied microorganisms, and hence provide validity to model simulations of more complex scenarios. This approach may therefore allow for inferring putative new interactions between the species forming the *in-silico* ecosystem of the human gut.

By integrating our bacterial community models with transcription data, we further demonstrated how we can identify transcriptional metabolic responses in each species for adaption to symbiotic conditions. By applying the two algorithms the mechanistic information was extracted from the transcriptome data compared with the study of Mahowald *et al.*³³. During the adaptation of *E. rectale* to presence of *B. thetaiotaomicron*, it was observed that the expression of *E. rectale*'s genes involved in the amino acid metabolism, TCA cycle and purine and pyrimidine metabolism were up regulated whereas genes involved in the degradation of carbohydrates are down regulated. Calculated Reporter Metabolite and subnetwork analysis supports this observation. During adaptation of *E. rectale* to presence of *B.*

thetaitaomicron it increased its dependency on the amino acid utilization, in particular glutamine that is the most abundant amino acid in the blood. Glutamine is a source of nitrogen and is used as a nitrogen donor for the biosynthesis of major biomass components e.g. nucleotides. Glutamine taken up by *E. rectale* is converted to glutamate and to other intermediates which are necessary for the synthesis of alanine, aspartate, arginine and proline. Previously the decreased blood level of glutamine in the PPAR- α null mouse which represents a number of discrepancies linked to diabetes and the metabolic syndrome⁴⁹ and the significantly greater portion Firmicutes species are reported in obese mice¹¹. Our results indicate that *E. rectale* in the gut may contribute to the decrease in the blood level of glutamine. The decreased glutamine level can be explained by the increased uptake of glutamine by Firmicutes species which is essential for increasing their growth.

During the adaptation of *B. thetaiotaomicron* to *E. rectale*, it increased its biomass depending on the polysaccharides. *B. thetaiotaomicron* yield energy for growth by fermenting non-digestible carbohydrates, e.g. cellulose, xylans, resistant starch and inulin in the colon and degrade these to SCFAs. The SCFAs produced from microbial fermentation can also be used as an energy substrate for host cellular metabolism.

Furthermore by mapping the flux distribution and expression data for two different conditions, significant enzymes with transcriptional regulation were identified which may further point to enrichment in activity of specific transcription factors. This type of analysis can be used to gain further insight into what drives the microbial ecosystem of the gut, and hereby assist with treatment of metabolic diseases that are associated with an altered gut microbiome.

The interest on the host-microbiota interactions and its health implications has been growing during the last years as demonstrated by several metagenomic studies of the human gut^{6,10,50}. Detailed mechanistic studies and generation of new hypothesis through genome-scale modeling is a necessary complement to the statistical correlations revealed by metagenomics studies. Our study demonstrated that the metabolic differences in the gut microbiota can be identified through genome-scale metabolic modeling of bacteria in the gut ecosystem and this may allow for facilitating rational design of prebiotics and probiotics and for development efficient treatment strategies for different disorders.

Methods

Reconstruction of GEMs for *B. thetaiotaomicron*, *E. rectale* and *M. smithii*. The *iEre400*, *iBth1201* and *iMsi385* were reconstructed based on *Eubacterium rectale* ATCC 33656⁵³, *Bacteroides thetaiotaomicron* VPI-5482⁵¹ and *Methanobrevibacter smithii* ATCC 35061³¹, respectively. The template models *iMH551*³⁷, *iAF1260*⁴⁶ and *iVS941*³⁸ were used for reconstruction of *E. rectale*, *B. thetaiotaomicron* and *M. smithii*. The GEMs are available at the Human Metabolic Atlas (www.metabolicatlas.com) in SBML format.

By default the lower and upper bounds for reactions were set to ± 1000 mmol/gDW⁻¹ h⁻¹, unless the reaction is irreversible. Following the RAVEN Toolbox for reconstruction the three template models were standardized based on databases with respect to metabolite names. The draft models were generated based on bi-directional BLASTp with respect to template models proteins and their orthologues in each interested species. The proteins were considered as orthologues with the settings of E-value < 10e - 30, sequence coverage > 50%, identity > 40% and alignment > 200 aminoacids. This gene mapping was controlled by identifying metabolic functions that were present in template models and not in draft models. Then the gaps were filled based on reference sequences database and literature. In addition a KEGG models for each species were generated by using RAVEN Toolbox and applied to fill the gaps in the draft models. The non-growth associated maintenance ATP were set based on available experiment data of the interested species or template model. The core biomass reactions adapted from the template models with respect to available information on biomass composition of the studied organisms.

Simulations of α and β problems. The available experimental data are given in concentrations per unit of cecal content and no information is available about the production rate of cecal content per unit of time. By dividing all the metabolic fluxes by the specific production rate of cecal content (which is equivalent to the dilution rate of a chemostat), we can formulate the problem in such a way that the output fluxes will have the units of concentration that are available experimentally (Figures 2.D & 3.D).



In the paper of Mahowald et al, the levels of colonization of the mice have been measured and reported as genome equivalents/gram weight cecal contents. This has been done for both mono and co-colonization. We extracted these data and converted them to gr D.w./gram weight cecal contents by considering the value of total dry weight per cell in *E. coli* which is $2.8e - 13$ gr. By considering the genome equivalent as a cell and multiplying the level of colonization with *E. coli* dry weight it is possible to calculate the concentrations per unit of cecal content. In the α -problem the objective function is minimizing the substrate uptake by constraining the biomass of single or community of species. In the β -problem the objective is maximizing the individual or community of species by constraining the substrate uptake. The optimization α & β problem solved therefore takes the following form:

$$\text{Minimize } Z = \frac{F_{\text{Substrate}}}{D} \quad (\alpha\text{-problem}) \quad \text{Maximize } Z = \frac{v_{\text{Biomass}_{ere,msi,bth}}}{D} \quad (\beta\text{-problem})$$

$$\frac{v_{\text{Biomass}_{ere,msi,bth}}}{D} = x_{ere,msi,bth} \quad (\alpha\text{-problem}) \quad \frac{F_{\text{Substrate}}}{D} = x_{ere,msi,bth} \quad (\beta\text{-problem})$$

$$\frac{F_{\text{Out}}}{D} = C$$

$$\frac{v_{\text{Prod}}}{D} = C + \left(\frac{K}{D}\right)C$$

$$s \cdot \bar{v} = \bar{\sigma}$$

D: Dilution rate

$\frac{K}{D}$: Ratio of SCFAs absorption

Prod: Butyrate, Acetate and Propionate

Reporter metabolites determination. Gene expression data generated by Mahowald et al³³, was downloaded from Gene Expression Omnibus with the accession number GSE14737. The data Cel-files were processed using R and Bioconductor. Data normalization was done by using Probe Logarithmic Intensity Error (PLIER) estimation. Differentially expressed genes were identified using the moderated t-statistic for pair-wise comparison. P-values were corrected for multiple testing by the method developed by Benjamini and Hochberg. The reporter metabolite algorithm was applied using an in-house developed software platform PIANO⁵². The algorithm makes use of p-values and the gene-metabolite associations to identify metabolites associated with transcriptionally changed genes.

Random sampling and transcriptional regulation identification. We have implemented a previously developed algorithm³⁵. In order to avoid loops in the solutions, the upper and lower bound were set to Inf and -Inf respectively instead of 1000 and -1000, which is a common practice. To set the problem for running random sampling algorithm the exchange fluxes were taken from solving the α -problem. In the case of *B. thetaiotaomicron*, the exchange fluxes from two solved α -problem where *B. thetaiotaomicron* is single and is together with *E. rectale* were used as input fluxes to the random sampling algorithm. The same procedure for the case of *E. rectale* was done.

- Backhed, F., Ley, R. E., Sonnenburg, J. L., Peterson, D. A. & Gordon, J. I. Host-bacterial mutualism in the human intestine. *Science* **307**, 1915–1920 (2005).
- Kinross, J. M., Darzi, A. W. & Nicholson, J. K. Gut microbiome-host interactions in health and disease. *Genome medicine* **3**, 14 (2011).
- Turnbaugh, P. J. et al. A core gut microbiome in obese and lean twins. *Nature* **457**, 480–484 (2009).
- Qin, J. J. et al. A metagenome-wide association study of gut microbiota in type 2 diabetes. *Nature* **490**, 55–60 (2012).
- Karlsson, F. H. et al. Gut metagenome in European women with normal, impaired and diabetic glucose control. *Nature* **498**, 99–103 (2013).
- Karlsson, F. H. et al. Symptomatic atherosclerosis is associated with an altered gut metagenome. *Nat Commun* **3**, 1245 (2012).
- Claesson, M. J. et al. Gut microbiota composition correlates with diet and health in the elderly. *Nature* **488**, 178–184 (2012).
- Qin, J. J. et al. A human gut microbial gene catalogue established by metagenomic sequencing. *Nature* **464**, 59–U70 (2010).
- Huttenhower, C. et al. Structure, function and diversity of the healthy human microbiome. *Nature* **486**, 207–214 (2012).
- Arumugam, M. et al. Enterotypes of the human gut microbiome. *Nature* **473**, 174–180 (2011).
- Turnbaugh, P. J. et al. An obesity-associated gut microbiome with increased capacity for energy harvest. *Nature* **444**, 1027–1031 (2006).
- Comalada, M. et al. The effects of short-chain fatty acids on colon epithelial proliferation and survival depend on the cellular phenotype (vol 132, pg 487, 2006). *J Cancer Res Clin* **133**, 211–211 (2007).
- Ruppin, H., Bar-Meir, S., Soergel, K. H., Wood, C. M. & Schmitt, M. G., Jr. Absorption of short-chain fatty acids by the colon. *Gastroenterology* **78**, 1500–1507 (1980).
- McNeil, N. I., Cummings, J. H. & James, W. P. Short chain fatty acid absorption by the human large intestine. *Gut* **19**, 819–822 (1978).

- McNeil, N. I. The contribution of the large intestine to energy supplies in man. *The American journal of clinical nutrition* **39**, 338–342 (1984).
- Dumas, M. E. The microbial-mammalian metabolic axis: beyond simple metabolism. *Cell metabolism* **13**, 489–490 (2011).
- Davie, J. R. Inhibition of histone deacetylase activity by butyrate. *J Nutr* **133**, 2485S–2493S (2003).
- Hamer, H. M. et al. Review article: the role of butyrate on colonic function. *Alimentary pharmacology & therapeutics* **27**, 104–119 (2008).
- Scheppach, W. & Weiler, F. The butyrate story: old wine in new bottles? *Current opinion in clinical nutrition and metabolic care* **7**, 563–567 (2004).
- Donohoe, D. R. et al. The warburg effect dictates the mechanism of butyrate-mediated histone acetylation and cell proliferation. *Molecular cell* **48**, 612–626 (2012).
- Duncan, S. H. et al. Human colonic microbiota associated with diet, obesity and weight loss. *Int J Obes (Lond)* **32**, 1720–1724 (2008).
- Wu, G. D. et al. Linking long-term dietary patterns with gut microbial enterotypes. *Science* **334**, 105–108 (2011).
- Faith, J. J., McNulty, N. P., Rey, F. E. & Gordon, J. I. Predicting a human gut microbiota's response to diet in gnotobiotic mice. *Science* **333**, 101–104 (2011).
- Mardinoglu, A. & Nielsen, J. Systems medicine and metabolic modelling. *Journal of internal medicine* **271**, 142–154 (2012).
- Lewis, N. E., Nagarajan, H. & Palsson, B. O. Constraining the metabolic genotype-phenotype relationship using a phylogeny of in silico methods. *Nature reviews. Microbiology* **10**, 291–305 (2012).
- Mardinoglu, A., Gatto, F. & Nielsen, J. Genome-scale modeling of human metabolism - a systems biology approach. *Biotechnology journal* **10.1002/biot.201200275** (2013).
- Ventura, M. et al. Genome-scale analyses of health-promoting bacteria: probionomics. *Nature reviews. Microbiology* **7**, 61–71 (2009).
- Stolyar, S. et al. Metabolic modeling of a mutualistic microbial community. *Molecular systems biology* **3**, (2007).
- Zomorrodii, A. R. & Maranas, C. D. OptCom: A Multi-Level Optimization Framework for the Metabolic Modeling and Analysis of Microbial Communities. *PLoS computational biology* **8**, (2012).
- Karlsson, F. H., Nookaew, I., Petranovic, D. & Nielsen, J. Prospects for systems biology and modeling of the gut microbiome. *Trends in biotechnology* **29**, 251–258 (2011).
- Samuel, B. S. et al. Genomic and metabolic adaptations of Methanobrevibacter smithii to the human gut. *Proceedings of the National Academy of Sciences of the United States of America* **104**, 10643–10648 (2007).
- Armougom, F., Henry, M., Vialettes, B., Raccach, D. & Raoult, D. Monitoring Bacterial Community of Human Gut Microbiota Reveals an Increase in Lactobacillus in Obese Patients and Methanogens in Anorexic Patients. *Plos One* **4** (2009).
- Mahowald, M. A. et al. Characterizing a model human gut microbiota composed of members of its two dominant bacterial phyla. *Proceedings of the National Academy of Sciences of the United States of America* **106**, 5859–5864 (2009).
- Patil, K. R. & Nielsen, J. Uncovering transcriptional regulation of metabolism by using metabolic network topology. *Proceedings of the National Academy of Sciences of the United States of America* **102**, 2685–2689 (2005).
- Bordel, S., Agren, R. & Nielsen, J. Sampling the solution space in genome-scale metabolic networks reveals transcriptional regulation in key enzymes. *PLoS computational biology* **6**, e1000859 (2010).
- Feist, A. M. et al. A genome-scale metabolic reconstruction for Escherichia coli K-12 MG1655 that accounts for 1260 ORFs and thermodynamic information. *Molecular systems biology* **3** (2007).
- Heinemann, M., Kummel, A., Ruinatscha, R. & Panke, S. In silico genome-scale reconstruction and validation of the Staphylococcus aureus metabolic network. *Biotechnology and bioengineering* **92**, 850–864 (2005).
- Kumar, V. S., Ferry, J. G. & Maranas, C. D. Metabolic reconstruction of the archaeal methanogen Methanosarcina Acetivorans. *BMC systems biology* **5**, (2011).
- Kanehisa, M., Goto, S., Sato, Y., Furumichi, M. & Tanabe, M. KEGG for integration and interpretation of large-scale molecular data sets. *Nucleic acids research* **40**, D109–D114 (2012).
- Henry, C. S. et al. High-throughput generation, optimization and analysis of genome-scale metabolic models. *Nature biotechnology* **28**, 977–U922 (2010).
- Agren, R. et al. The RAVEN toolbox and its use for generating a genome-scale metabolic model for Penicillium chrysogenum. *PLoS computational biology* **9**, e1002980 (2013).
- Heinken, A., Sahoo, S., Fleming, R. M. & Thiele, I. Systems-level characterization of a host-microbe metabolic symbiosis in the mammalian gut. *Gut microbes* **4**, 28–40 (2013).
- Salyers, A. A., O'Brien, M. & Kotarski, S. F. Utilization of Chondroitin Sulfate by Bacteroides-Thetaiotaomicron Growing in Carbohydrate-Limited Continuous Culture. *J Bacteriol* **150**, 1008–1015 (1982).
- Barcenilla, A. et al. Phylogenetic relationships of butyrate-producing bacteria from the human gut. *Applied and environmental microbiology* **66**, 1654–1661 (2000).
- Pavlostathis, S. G., Miller, T. L. & Wolin, M. J. Cellulose Fermentation by Continuous Cultures of Ruminococcus-Albus and Methanobrevibacter-Smithii. *Applied microbiology and biotechnology* **33**, 109–116 (1990).



46. Munoz-Tamayo, R., Laroche, B., Walter, E., Dore, J. & Leclerc, M. Mathematical modelling of carbohydrate degradation by human colonic microbiota. *J Theor Biol* **266**, 189–201 (2010).
47. Samuel, B. S. & Gordon, J. I. A humanized gnotobiotic mouse model of host-archaeal-bacterial mutualism. *Proceedings of the National Academy of Sciences of the United States of America* **103**, 10011–10016 (2006).
48. Lin, H. V. *et al.* Butyrate and propionate protect against diet-induced obesity and regulate gut hormones via free fatty acid receptor 3-independent mechanisms. *Plos One* **7**, e35240 (2012).
49. Atherton, H. J. *et al.* A combined ¹H-NMR spectroscopy- and mass spectrometry-based metabolomic study of the PPAR-alpha null mutant mouse defines profound systemic changes in metabolism linked to the metabolic syndrome. *Physiological genomics* **27**, 178–186 (2006).
50. Structure, function and diversity of the healthy human microbiome. *Nature* **486**, 207–214 (2012).
51. Xu, J. *et al.* A genomic view of the human-Bacteroides thetaiotaomicron symbiosis. *Science* **299**, 2074–2076 (2003).
52. Våremo, L., Nielsen, J. & Nookaew, I. Enriching the gene set analysis of genome-wide data by incorporating directionality of gene expression and combining statistical hypotheses and methods. *Nucleic acids research* (2013).

Acknowledgements

We are grateful to Prof. Fredrik Bäckhed and Dr. Petia Kovatcheva from Göteborg University for helpful discussion and sharing information about the gut microbiome. This

project was supported by Knut and Alice Wallenberg Foundation, Tore Nilsons Stiftelse för Medicinsk Forskning, Chalmers University of Technology Foundation and Torsten Söderbergs stiftelse.

Author contributions

S.S. and J.N. designed the study. S.S. reconstructed the models for ere and msi, performed modeling and transcriptome analysis. F.K. reconstructed the model for bth and assisted with analysis. S.B. assisted with metabolic modeling. I.N. and A.M. assisted with transcriptome data analysis. J.N. conceived the project. S.S. and J.N. wrote the manuscript and all authors read and approved the final manuscript.

Additional information

Supplementary information accompanies this paper at <http://www.nature.com/scientificreports>

Competing financial interests: J.N. is a shareholder of MetaboGen AB. All the other authors declare no conflict of interest.

How to cite this article: Shoaie, S. *et al.* Understanding the interactions between bacteria in the human gut through metabolic modeling. *Sci. Rep.* **3**, 2532; DOI:10.1038/srep02532 (2013).



This work is licensed under a Creative Commons Attribution 3.0 Unported license. To view a copy of this license, visit <http://creativecommons.org/licenses/by/3.0>